Estimation of components of energy balance on drifting ice over Arctic Ocean

BIAN Lingen(卞林根)[1]**, LU Longhua(陆龙骅)[1], GAO Zhiqiu(高志球)[1]
CHENG Yanjie(程彦杰)[1], LU Changgui(逯昌贵)[1] and LI Shiming(李诗明)[2]

1. Chinese Academy of Meteorological Sciences, Beijing 100081, China
2. National Research Center for Marine Environment Forecast, Beijing 100081, China

Received September 13, 2000; revised November 10, 2000

Abstract Estimation and simulation were carried out for the components of ice-surface energy balance and turbulent exchange parameters using the flux-profile method and the simple biosphere model version 2 (SiB2, hereinafter) respectively based on the measured results for the atmosphere in the near-ice-surface layer, which were observed by the First Arctic Scientific Expedition of China in August, 1999 at a joint ice-research station (75°02′N, 160°51′W) on the drifting ice of Arctic Ocean. Evidence suggests that during the melting period of drifting ice the sum of the ice-released sensible heat and effective melting-consumed heat is greater than the net ice-absorbed radiation on the surface, with the excess heat coming via heat conduction from the deep layers of the ice mass. The simulated net radiation is systematically 18% greater than the measured results, while the simulated sensible heat flux is systematically 3% lower than the measured ones; and the simulated ice-surface heat flux differs noticeably from its calculation. Hence, we see that although the measured sequences are short, the simulations of net radiation and sensible heat fluxes by the SiB2 model are comparatively good, the simulation of other forms of fluxes still needs to be improved.

Keywords: Arctic drifting ice, energy flux, calculation and simulation.

In the study of the effect of the ocean-ice-atmosphere interactions and their feedback mechanism on global climate[1,2] one of the major problems of scientific interest is to determine the parameters of momentum, energy and vapor exchange in the atmospheric boundary layer. Due to the northernmost geography and adverse environment of the Arctic Ocean, boundary-layer observations are lacking in this region. Badgley[3] investigated the annual variation features of components of the energy balance. Lindsay[4] analyzed and simulated the time-dependent variation in such components over the Arctic drifting ice surface by virtue of 45-year meteorological data obtained from the station of the former USSR, and suggested that the ice melting plays a role of effective heat consumption. Meesters[5] researched the profiles and turbulent fluxes in the near-surface layer over the flat and melting ice in Greenland. Handorf[6] studied the turbulent transfer over the Antarctic sea ice surface, focusing on quantifying the actual balance height of a steady atmospheric boundary layer, and indicated that atmospheric stability has to be considered in the relations between parameters. Johannessen[7] discussed the possible effects of the trend of Arctic ice size shrinking on the climatic variation. Bian[8] investigated the annual variation in the components of surface energy balance over the Antarctic coastal area,

* Project supported by the National Natural Science foundation of China (Grant No. 49975006) and the National Program of Arctic Scientific Expedition.

** E-mail: bianlingen@sina.com.cn.

and compared the results with those of the Arctic counterparts studied by Badgley[3]. Internationally, some studies have been reported on the Arctic ocean ice-cover-air interactions and the physical processes in the boundary layer, but there is still controversy over the research results, such as the rational determination and parameterizations of the valu of momentum, heat and vapor exchange. All these need to be quantified with the aid of further observational facts and relevant analysis.

Using the observation data from the Arctic joint station in August, 1999 about such parameters as temperature, humidity, wind profile and components of radiation balance in the near-ice-surface layer, and adopting the profile method, we calculated the components of energy balance equation, and simulated the components of the energy balance equation in the period of August 19 ~ 24 by SiB2 model with the ice cover considered as the underlying surface (regardless of the presence of vegetation). This approach may serve as a reference for the research of a boundary-layer parameterization scheme for the Arctic Ocean.

1 Measurements

A joint-ice-research station was constructed on a quite plain drifting ice with multi-year history, 4 m in depth and 0.5 km^2 in area. 50% ~ 70% of the surrounding region was drifting ice, and sometimes the station was encircled by floe driven by winds and oceanic current. The scope under observation had the characteristics of high-latitude ice lumps in their melting, i.e. the surface is snow-free on the whole, grayish and opaque owing to melting and freezing.

The meteorological tower was 8 m high. Sensors of temperature, humidity and windspeed were mounted 0.5, 4 and 8 m above the surface for gradient observations and that of wind direction was installed at the top of the tower. The upward and downward radiometers were fixed on a 1.5 m high mast to measure the global and reflected radiation of the ice surface, and upwelling and downwelling long-wave radiation. In order to obtain ice temperature profile, three temperature sensors were set at the depths of 0.1, 0.2 and 0.4 m in the ice, respectively, while a temperature sensor was set at the ice surface. Before setting, the instruments and sensors were calibrated against the standards in the metering station of China Meteorological Administration. The Arctic observations were undertaken from 00:00 (local time) of August 19 to 16:00 of August 24, 1999. Continuous series of meteorological data of 10-min means, and synchronous visual data of cloudiness, cloud forms, visibility and weather phenomena were obtained.

2 Calculation schemes

The energy balance equation at the ice surface can be written in the form[4]

$$R_n = H + LE + G + M, \tag{1}$$

where R_n is the net radiation calculated out with up- and downward long- and short-wave radiation using the relationship $R_n = S_t - S_g + L_a - L_g$ (S_t is the solar short-wave radiation, S_g the reflected short-wave radiation from ice surface, L_a the longwave radiation down from the atmosphere, and L_g the longwave (infrared) radiation emitted up from the ice surface), H the sensible heat flux, LE the latent heat flux, G the ice heat flux and M the effective heat flux for ice melting, which could be acquired from the gradient observations, flux-profile method and simulation.

2.1 Profile technique for turbulent flux

There are many turbulent flux measuring and calculating schemes. Here we adopt the widely-used aerodynamic method. By virtue of Monin-Obukhov similarity theory[9] and with the known flux-profile relation[10], we obtained the frictional wind u_*, characteristic temperature T_*, characteristic humidity q_* and Monin-Obukhov stability length L using the iteration method. The fluxes of H and LE are

$$H = -\rho C_p u_* T_*, \tag{2}$$

$$LE = -\rho L_V u_* q_*, \tag{3}$$

where ρ represents the density of atmosphere in the near-surface layer, L_v the coefficient of latent heat of evaporation at 0℃ and C_p the specific heat of moisture air at constant pressure.

2.2 Calculation scheme of ice heat flux

After temperatures of the ice surface and several depths inside are found, the force-restoring method is employed to examine the ice heat flux[11]

$$G = C_{GA}\left(\frac{\partial T_G}{\partial t}\right) + 2\pi \frac{C_{GA}}{\Gamma}(T_G - T_M), \tag{4}$$

where Γ denotes the period of the daily cycle ($\Gamma = 24 \times 3600$ s), T_G the ice-surface temperature, T_M the deeper ice temperature, ice heat capacity per unit area $C_{GA} = C_G \times d_s$(J/m^{2}K)[1] with C_G(= 2.05×10^6 J/m^{3}K)[12] as the volumetric heat capacity and $d_s = [(\gamma_g \Gamma)/(4\pi)]^{1/2}$ as the effective ice depth that can sense the diurnal cycle, γ_g(= 0.92×10^{-6} m^2/s) the ice heat diffusivity[13], $C_{GA}\left(\frac{\partial T_G}{\partial t}\right)$ the ice surface response to the net radiation and $2\pi \frac{C_{GA}}{\Gamma}(T_G - T_M)$ the thermal conduction between the surface and the deeper ice layer for heat exchange balance.

2.3 Calculation of heat absorption in melting

An ice-snow surface differs from that of soil. It has melting and condensation. So there is difference in the heat balance expression between them. When the ice surface is warmer than its melting point, the melting-absorbing heat M is expressed as $M = C_G(T_i - T_{mi})/\Delta t$, where T_{mi} is the melting point temperature depending strongly on ice salinity, about which Lindsay gave a detailed description[5], and $T_{mi} = 273.16 - 0.05411S$ with S as the ice salinity in units of g/kg), C_G is the volumetric heat capacity of ice based on a 10-min mean sample. For $\Delta t = 600$ s, M is obtained by calculating the temperatures (T_i) of all the sampled levels.

2.4 Application of the model SiB2

The SiB2 model developed by Sellers et al.[14] serves to simulate the interactions between

1) 10^6J = 11.57 W

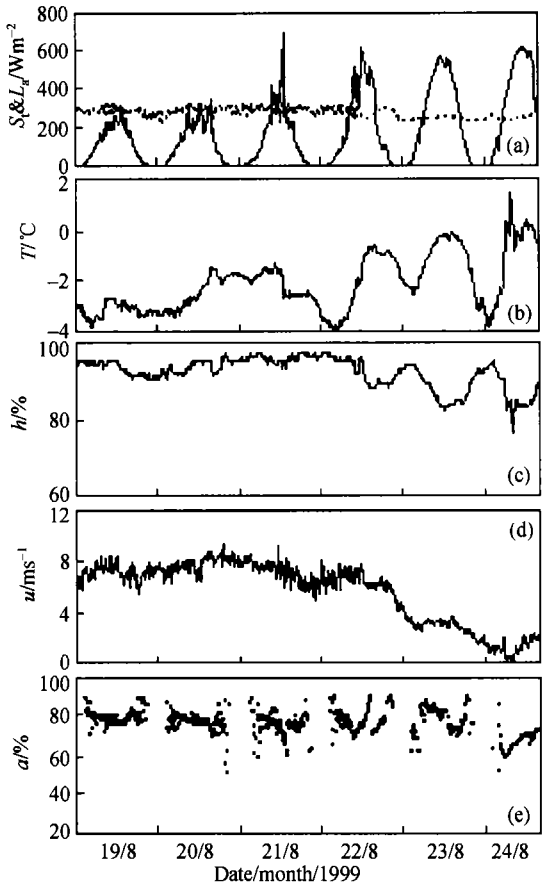

Fig. 1 Time series of 10-min mean of downward radiation (solid line: shortwave S_t and dot line: longwave L_a(a)), air temperature T(b), relative humidity h(c), horizontal wind u (d), and ice-surface albedo α(e), for August 19 ~ 24, 1999.

air and a range of underlying surfaces (including the biosphere) to get quantities of sensible and latent heat fluxes, surface temperature, aerodynamic resistance and others. These boundary-layer processes are investigated largely by means of a two-stream approximate radiative transfer model to get the up- and downward radiation fluxes, and the five components of incoming radiation, i.e. those of visible (diffuse and direct), near infrared (diffuse and direct), and infrared radiation. Surface albedo and net radiation absorption are parameterized to be a function of solar elevated angle, atmospheric and surface properties.

The six forcing variables to be inputted into the SiB2 consist of downward short radiation S_t, and long-wave radiation L_a, humidity h, air temperature T, horizontal wind u and precipitation R. The former five variables are from the *in situ* measurements as shown in Fig. 1. During the observation period snowfall happened occasionally, but the precipitation was also almost zero. Fig. 1 includes surface albedo owing to its importance. Fig. 1 shows that even it was near the polar-day period, the high-latitude zone was dominated by low temperature and high humidity. From the observation of about 6 days, the downward radiation was found to be 2 ~ 3 times higher in the fine days than in the overcast days; the maximum downward radiation on clear days exceeded 600 Wm^{-2} as compared to ~ 200 Wm^{-2} on overcast days; the downward long-wave radiation showed no big difference in both cases, reaching the order of 300 Wm^{-2} and dropping slightly with the reduced humidity in the fine days; the ice surface albedo varied little for strong winds and low temperature, attaining roughly 0.8 for low winds in the fine days; when the temperature rose and the ice surface began to thaw, the albedo was somewhat reduced.

3 Discussion

Setting the albedo and emission of the near infrared band radiation from the ice surface to be 0.70 and 0.97, respectively, we simulatied the net radiation R_n, sensible heat flux H, latent heat flux LE for the surface, ice heat flux G, and effective radiation temperature.

3.1 Net radiation

Figure 2 shows a comparison between the observed (or calculated by flux profile method) and

simulated (by SiB2) energy balance components, including net radiation, sensible heat flux, latent heat flux, ice heat flux and melting-absorbed heat flux. The net radiation values are shown in Fig.2 (a), the phases of the daily cycle of the observed and simulated values are in rough agreement, with the maximum (minimum) in the midday (nocturnal) hours of the area. The simulated values are bigger (smaller) than the observed values in the daytime (nighttime). The 6-day time series of the simulated net radiation has systematic errors (Fig.3 (a)); that is, the simulated values are overestimated by 18% on average, as compared with the observed ones ($R_{nm} = 0.82R_{no}$), whereas the size of samples is 816 with the correlation coefficient of 0.85. The values of daily mean total are 2.5 and 0.9 MJm^{-2} from the simulations and observations respectively, and the difference maybe arises from the fact that the SiB2 took no sufficient account of the interactions between the sea with or without floe, and the atmosphere. The setting of the constants of the radiation equation is based on the condition of vapor, the temperature of the air and the properties of the underlying surface, particularly the climatic features of low temperature and high humidity of the target ocean.

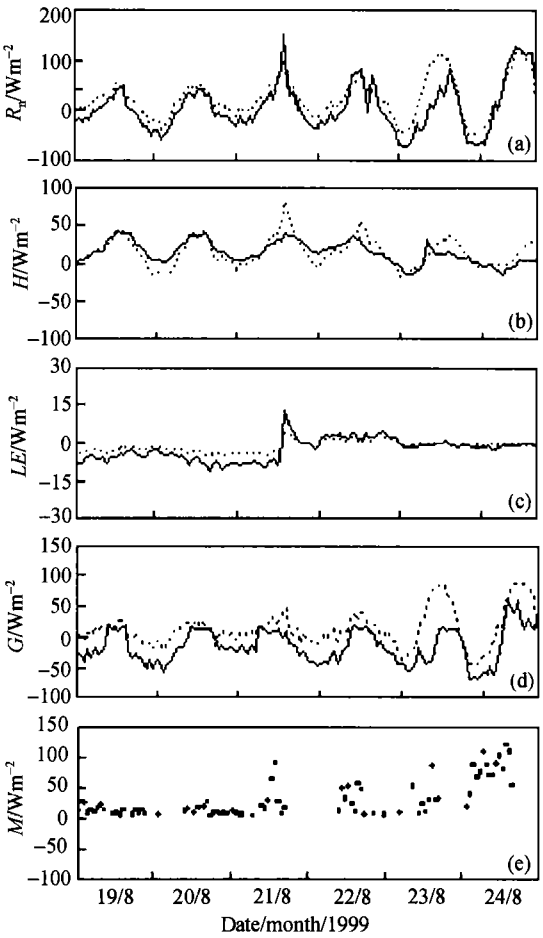

Fig. 2 Comparison between the simulated (dot line) and observed or calculated (solid line) values of the net radiation (a), sensible heat flux(b), latent heat flux(c), ice heat flux (d) and melting absorbed heat flux(e).

3.2 Turbulent heat flux

A comparison between the simulated and the calculated values of sensible heat flux is given in Fig. 2(b); the former is by 3% ($H_m = 1.03H_p$) lower than the latter. Their phases are in rough agreement, and their daily variations are pronounced with a correlation coefficient of 0.95 (Fig. 3(b)), showing that the SiB2 can well imitate the sensible heat flux, giving a the daily mean total of 1.26 MJm^{-2} for the 6-day experiment rather than 1.14 MJm^{-2} from the calculations. Because the temperature of ice surface was higher than the melting point, there occurred melting, which was not included in the model, so the simulated sensible heat flux is greater than the calculated one. On the other hand, as evidenced from Fig.2(c), both the simulated and calculated latent heat fluxes are quite small, displaying no remarkable daily variation, and the latent heat was negative-valued in most of the period over the ice surface owing to the moist advection from the sea. On the fourth day of the observation the ice surface began to melt because the sea around the station was floe-covered and the winds were slightly mitigated, which increased the humidity on ice surface, leading to positive value of the calculated latent heat flux. Because no melting

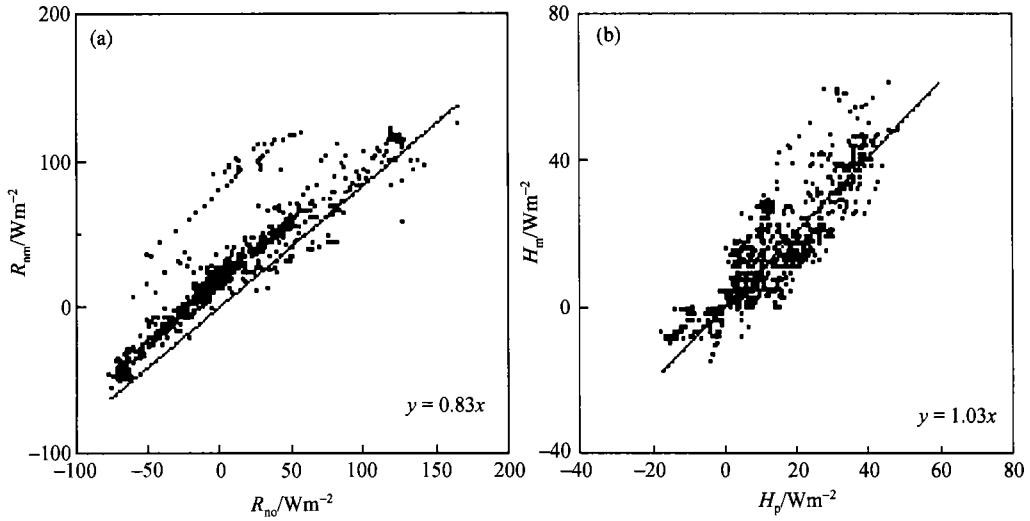

Fig. 3 Simulated results of net radiation (R_{nm}) versus the observed net radiation (R_{no}) (a), and the simulated sensible heat flux (H_m) versus the calculated analog (Hp) (b).

is considered in the model, the simulated latent heat flux differs from the calculated one, with the simulated daily mean total of -0.11 versus -0.21 MJm^{-2} from calculations. It seems that the effects of negative latent heat flux have to be considered when we investigate the contribution of latent heat transfer to air in the floe area.

3.3 Ice heat flux and melting absorbed heat

Part of the ice-absorbed net radiation in the daytime serves to heat the atmosphere in turbulent form, the rest is consumed to melt ice or go into the deep of ice-body. The nocturnal radiative cooling offsets the ice-liberated heat flux. For short of equipment, we did not measure the temperature inside the ice body below 40 cm so some errors are possible. From the temperature profile (Fig. 4) we notice that the temperature at 40 cm depth has no change, nor experiences diurnal variation at all, showing that this layer is a mixed one of the heat exchange between the upper and lower level. The simulated and estimated ice heat fluxes in a daily cycle are shown in Fig. 2(d) and the daily total averages of 6 days are 1.42 and -1.40 MJm^{-2}. They differ greatly, which is possibly because this model took no account of the permeation of melted liquid into the ice depth, which might alter the properties of thermal conduction therein.

The calculated absorbed melting-heat is given in Fig. 2(e). During the 136 hours of observation, the ice temperature was above the melting point for 56 hours. In the noon hours of 19 ~ 20, August, it was overcast, so the consumed melting-heat was not remarkable. But in the midday hours of August 21, strong net radiation emerged over the ice and the maximum heat consumption for melting was observed. In the afternoon of August 22 the sky was clear, leading to stronger ice surface melting due to the intensive solar radiation and the effective energy consumption reached >100 Wm^{-2}. The consumption of heat is therefore more significant in fine days than in overcast weather and the daily total was 1.27 MJm^{-2} averaged over the 6 days. Thus the consumption melting-energy is an important

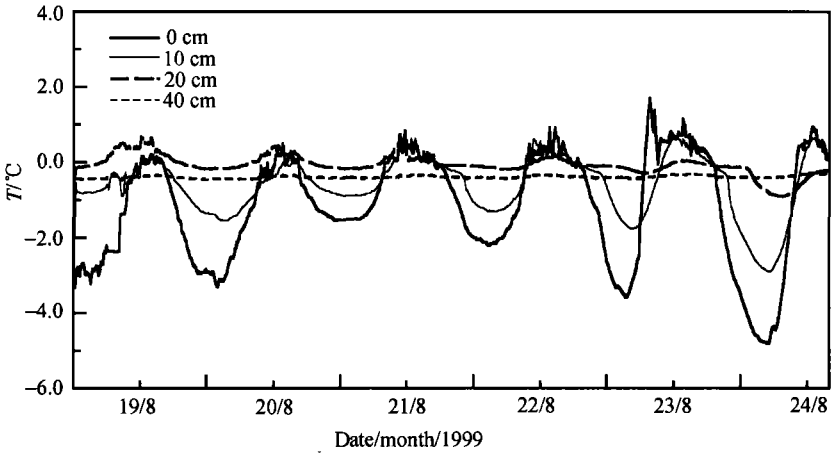

Fig.4 Time series of ice temperature for August 19 ~ 24, 1999.

component of energy balance in the target region. The melting of ice was not included in the SiB2 model and the left-over part after subtraction of sensible and latent heat from the net radiation was taken as the ice heat flux, thus resulting in a bigger difference between the simulation and calculation of ice heat flux.

3.4 Turbulent exchange coefficients

Figure 5(a) depicts the atmospheric stability parameters Ri and z/L for the 136 hourly samples based on the flux-profile calculations for the Arctic plain ice surface. Except few of the absolute values of Ri and z/L were greater than 0.1, most of them were smaller than 0.05 or close to zero. It indicates that atmospheric stratification on the floe region was near neutral and has quite weak turbulent exchange even in fine weather during the polar-day period. Fig.5(b) shows the time series of turbulent exchange coefficients of calculated momentum (C_D) and heat (C_H). We can see that very few of the values are related to atmospheric stability, and the others range over $0.5 \times 10^{-3} \sim 2 \times 10^{-3}$. As a result, $C_{DN} = 1.24 \times 10^{-3}$ and $C_{HN} = 1.12 \times 10^{-3}$ are obtained for the near neutral stratification ($Ri \approx 0$ and $z/L = 0$). A long-term research of on-ice energy budget in the Arctic Ocean Lindsay[5] used the exchange coefficients of 2.30×10^{-3} for both heat and vapor in the near neutral stratification. These coefficients as well as the calculated sensible and latent heat fluxes are roughly two times as great as those found by us in the experiment. In the observation we obtained C_{DN} and C_{HN} for winds at 2 ~ 9 m/s over the flat floe, which are typical results for the Arctic Ocean. Those values are smaller than $C_{DN} \approx 2 \times 10^{-3}$ (for flat land) and greater than $C_{DN} \approx 1 \times 10^{-3}$ (over sea). In view of the limited number of observations made in the floe zone, the observed values of the two parameters differ noticeably. They were obtained in different observational experiments. This is a problem to be resolved by longer observations of the atmospheric boundary layer over the Arctic Ocean in future.

5 Conclusion remarks

The 6-day simulated energy balance components over the Arctic floe area indicate that the SiB2

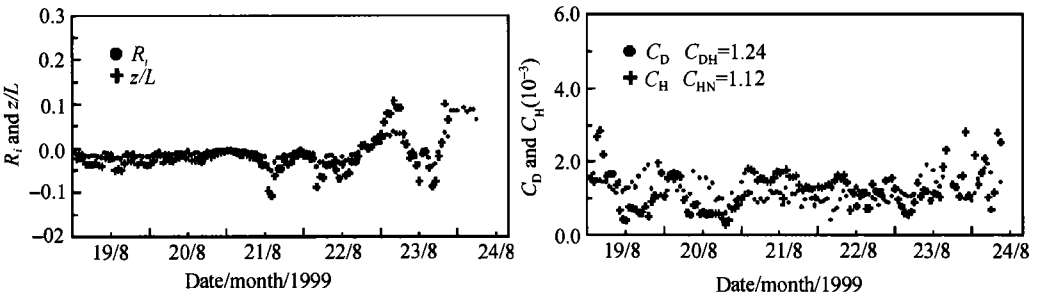

Fig. 5 Time series of Ri and z/L (a) and C_D and C_H(b) for August 19 ~ 24, 1999.

is good for simulating the net radiation and sensible heat flux but is poor for ice heat flux and latent heat flux. Because the ice melting is not considered, the closing error between the simulated $H + LE + G$ and the measured net radiation is quite large, whereas the difference is relatively small between the calculated $H + LE + G + M$ from the flux-profile scheme, the ice heat flux and consumed melting heat equations and the measured daily total of net radiation. The maximum(minimum) difference ΔR_n ($R_n - (H + LE + G + M)$) is 15%(8%), averaging 11%. If we consider the accumulated errors arising from the observing instruments and calculation, they are relatively rational. The heat balance components of Arctic floe vary in the following manner.

(i) Ice-released sensible heat and effective heat consumption in melting are greater in value than ice-absorbed net radiation with the excess of energy coming dominantly via the conduction of heat from the depth of ice to its surface. The melting-consumed effective energy is an important parameter in dealing with the heat balance over the floe region and is of the same order of magnitude as that of sensible heat flux.

(ii) The negative latent heat flux over the floe in most of the observations is associated with the moist advection from the ice-free sea. "Humidity inversion" disappears and positive latent heat flux emerges when the station is surrounded by drifting ice over several kilometers around. Because the temperature was around 0℃ during observation, the rates of evaporation and condensation were low, implying that their fluxes were small.

(iii) The near ice-surface layer atmosphere is in a neutral stratification. The weakly unstable or stable stratification was developed only for a short time in fine weather. The exchange coefficients of momentum and heat are 1.24×10^{-3} and 1.12×10^{-3}, respectively, in the near neutral stratification.

References

1 First Arctic Research Expedition of China. Arctic Scientific Expedition Report(in Chinese), ed. Bai, Y., Beijing: China Ocean Press, 1999, 1 ~ 55.

2 National Snow and Ice Data Center (NSIDC), Arctic Ocean Snow and Meteorological Observations From Russian Drifting Stations. Boulder: University of Colorado, CO.CD-ROM, 1996.

3 Badgley, F. I. Arctic heats budget and atmospheric circulation. On Arctic heat budget and atmospheric circulation. Santa Monica. In: Proceedings of the symposium, The Raand Corporation, 1996, 268.

4 Lindsay, R. W. Temporal variability of the energy balance of thick arctic pack ice. Journal of Climate, 1998, (11): 313.

5 Meesters, E. A. C. Turbulence observations above a smooth melting surface on the Greenland ice sheet. Boundary-Layer Meteorology, 1997, (85): 81.
6 Handorf, D. et al. The stable atmospheric boundary layer on Antarctic ice sheet. Boundary-Layer Meteorology, 1999, 91: 164.
7 Johannessen, O. M. The Arctic shrinking sea ice. Nature, 1995, 361: 335.
8 Bian, L. et al. Observational study of annual variation of surface energy balance components at Zhongshan station of Antarctica. Science in China, Series B, 1992, 36(8): 976.
9 Monin, A. S. et al. Basic laws of turbulent mixing in the atmosphere near the ground. Tr. Akad. Nauk SSSR Geophyz. Inst., 1954, 24(151): 162.
10 Businger, J. A. et al. Flux profile relationships in the atmospheric surface layer. J. Atmos. Sci., 1971, 28: 181.
11 Zhang, D. et al. A high-resolution model of the planetary boundary layer-sensitivity tests and comparisons with SESAME-79 data. J. Appl. Meteor., 1982, 21: 1594.
12 Stull, R. B. An introduction to Boundary Layer Meteorology, London: Kluwer Academic Publishers, 1984, 642 ~ 643.
13 Ono, N. Specific heat and heat of fusion of sea ice. Physics of Snow and Ice, H. Oura. ED., Hokkaido: Institute of Low Temperature Science, 1967, 599 ~ 610.
14 Sellers, P. J. et al. A revised land surface parameterization (SiB2) for atmospheric GCMs. Part I: Model formulation. Journal of Climate, 1996, 9: 675.